

Low-power, fast, selective nanoparticle-based hydrogen sulfide gas sensor

William Mickelson, Allen Sussman, and Alex Zettl

Citation: *Appl. Phys. Lett.* **100**, 173110 (2012); doi: 10.1063/1.3703761

View online: <http://dx.doi.org/10.1063/1.3703761>

View Table of Contents: <http://apl.aip.org/resource/1/APPLAB/v100/i17>

Published by the [American Institute of Physics](#).

Related Articles

Upgrading the sensitivity of spectroscopy gas analysis with application of supersonic molecular beams
J. Appl. Phys. **111**, 074903 (2012)

Response to "Comment on 'GaSe_{1-x}S_x and GaSe_{1-x}Te_x thick crystals for broadband terahertz pulses generation'" [*Appl. Phys. Lett.* **100**, 136103 (2012)]
Appl. Phys. Lett. **100**, 136104 (2012)

Investigation of the physics of sensing in organic field effect transistor based sensors
J. Appl. Phys. **111**, 044509 (2012)

ZnO coated nanospring-based chemiresistors
J. Appl. Phys. **111**, 044311 (2012)

Tracer-encapsulated solid pellet injection system
Rev. Sci. Instrum. **83**, 023503 (2012)

Additional information on *Appl. Phys. Lett.*

Journal Homepage: <http://apl.aip.org/>

Journal Information: http://apl.aip.org/about/about_the_journal

Top downloads: http://apl.aip.org/features/most_downloaded

Information for Authors: <http://apl.aip.org/authors>

ADVERTISEMENT



ACCELERATE AMBER AND NAMD BY 5X.
TRY IT ON A FREE, REMOTELY-HOSTED CLUSTER.

LEARN MORE

Low-power, fast, selective nanoparticle-based hydrogen sulfide gas sensor

William Mickelson,^{1,a)} Allen Sussman,^{1,2} and Alex Zettl^{1,2,3,a)}

¹Center of Integrated Nanomechanical Systems, University of California at Berkeley, Berkeley, California 94720, USA

²Department of Physics, University of California at Berkeley, Berkeley, California 94720, USA

³Materials Sciences Division, Lawrence Berkeley National Laboratory, Berkeley, California 94720, USA

(Received 2 February 2012; accepted 27 March 2012; published online 25 April 2012)

We demonstrate a small, low-cost, low-power, highly sensitive, and selective nanomaterials-based gas sensor. A network of tungsten oxide nanoparticles is heated by an on-chip microhotplate while the conductance of the network is monitored. The device can be heated with short pulses, thereby drastically lowering the power consumption, without diminishing the sensor response. The sensor shows high sensitivity to hydrogen sulfide and does not have significant cross sensitivities to hydrogen, water, or methane, gases likely to be present in operation. A sensing mechanism is proposed, and its effect on electronic properties is discussed. © 2012 American Institute of Physics. [<http://dx.doi.org/10.1063/1.3703761>]

Real-time monitoring of pollutant, toxic, and flammable gases is important for health and safety of industrial workers and the general population. Small, lightweight, fast, low-power, low-cost sensors enable ubiquitous monitoring of these gases, allowing for prevention of exposure or explosions, as an aid in rapid response to hazardous leaks.¹ Currently, there are many methods of detecting such gases, but most available sensors suffer from slow response times, high power consumption, high cost, and/or inability to operate in harsh conditions.^{2,3}

Hydrogen sulfide was chosen as an example analyte to demonstrate this detection method due to its toxicity at low concentrations. However, the detection platform could be adapted to other analytes of interest by choosing appropriate nanoparticle chemistries. Hydrogen sulfide is a naturally occurring gas found in oil deposits and natural gas fields. It is extremely toxic at concentrations as low as hundreds of parts per million. However, its concentration in natural gas can be up to 90%.⁴ Workers may be exposed to H₂S in many industrial processes (oil and natural gas drilling and refining, sewage treatment, paper milling, and many others). It is potentially lethal in concentrations as low as 320 ppm, and it is also flammable, corrosive, and low-lying so that high concentrations may develop over time.^{5,6} Although H₂S can be detected by the human nose at levels as low as 0.5 ppb, for concentrations above 100–150 ppm (the concentration around which H₂S begins to have damaging health effects), H₂S paralyzes the olfactory nerve after a few inhalations, disabling the sense of smell.⁶ Appropriate personal monitoring of H₂S in industrial situations is critical to worker safety.

Current state-of-the-art detection of H₂S is typically achieved using electrochemical cells, semiconducting metal-oxide (SMO) sensors, or photoluminescence sensors. Electrochemical cells are sensitive, selective, and low power, but they are expensive and can fail in high heat or extreme humidity, making them non-ideal for use in many harsh environments.^{2,3} Conventional SMO sensors have a simple

design, fast response time, long lifetime, and can operate in a wide temperature range, but consume watts of power making personal and mobile monitoring difficult.⁷ Sensors that operate on the principle of photoluminescence are not affected by temperature or humidity, but they are large, high power, and expensive.³

Nanostructures have received considerable attention as sensing elements.⁸ Nanostructures have large surface area to volume ratios enhancing the effect surface states have on the bulk electronic properties. The low thermal mass of nanomaterials also enables heating to high temperatures with low power. Nanostructured gas sensors are amenable to fabrication on silicon wafers and therefore can take advantage of the highly developed nature of silicon process technology.⁹ Much of the research into nanomaterials-based sensors has focused on SMO sensors^{10–13} since SMO sensors are a proven technology and have high chemical versatility. Tungsten oxide has been shown previously to be sensitive to H₂S.^{14–18} However, the reported response times of these sensors range from a few to many minutes, which is unacceptable for many applications, and there is cross sensitivity to other gases such as hydrogen.¹⁶

Here we report on H₂S sensors made from networks of WO₃ nanoparticles fabricated with on-chip microhotplates,^{19–21} which are fast, sensitive, low-power, and manufacturable at low cost. These sensors have a limit of detection below 1 ppm, a measurement range from 0–200 ppm, low cross sensitivity to common gases, response times of only a few seconds, and can operate at low power (<10 mW).

To fabricate the WO₃ nanoparticle-based H₂S sensor, the WO₃ nanoparticles of nominal size 90 nm (MKNano, MKN-WO3-090) are suspended in isopropanol via ultrasonication and are either drop cast or spin cast onto the microhotplate device (Kebaili Corporation, KMHP-100), as shown in Fig. 1(a). The microhotplate device, shown in Fig. 1(b), consists of a film of silicon nitride (500 μm × 500 μm × 500 nm), a serpentine heating element (250 μm × 250 μm) made of platinum that is 10 μm wide and 250 nm tall, followed by a 500-nm-thick layer of SiO₂ to isolate the heater from the

^{a)}Authors to whom correspondence should be addressed. Electronic addresses: wmickelson@berkeley.edu and azettl@physics.berkeley.edu.

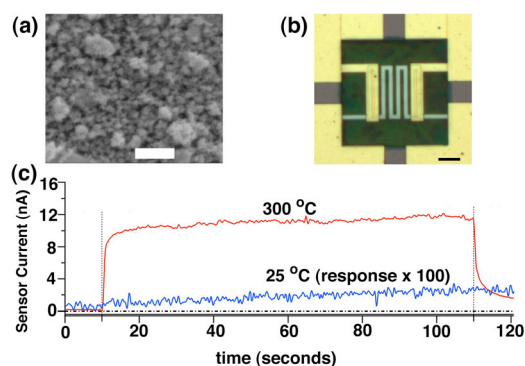


FIG. 1. (a) SEM image of WO_3 nanoparticles deposited on a substrate. Scale bar is 500 nm. (b) Optical image of microhotplate. The Pt heating element is suspended on a 500-nm-thick silicon nitride membrane. A 500-nm-thick SiO_2 insulating layer separates the gold lead electrodes from the Pt heating element. Scale bar is 100 μm . (c) WO_3 nanoparticle sensor current at room temperature (blue, lower) and 300 °C (red, upper) to a 100-s-long exposure.

sensing element. Two gold electrodes, 250 μm wide and 200 μm apart, are the source and drain contacts for the sensing element.

Hydrogen sulfide gas is delivered to the sensor by a computer-controlled gas delivery system. A cylinder of 500 ppm H_2S , balanced in N_2 , is diluted via mass flow control with air, which has been dried with pressure swing adsorption dryers and passed through an activated carbon scrubber to remove hydrocarbons and other contaminants. The gas stream can also be humidified by means of a controlled evaporator mixer. Interfering gases can also be introduced into the gas stream. The stream of gas is continuously delivered to the sensor, after which it flows to a humidity sensor (Vaisala HUMICAP HMT330), and a H_2S reference sensor (Teledyne API 101E). Sensor and heater voltage is sourced, and current measurements are taken by a Keithley 2602A, which is controlled by Zephyr,²² an open-source Java-based instrument control and measurement software package. Zephyr is also used to acquire all data from the source-measure unit, the reference sensors, and the gas delivery system.

The response of the WO_3 nanoparticle network sensor to H_2S exposure is shown in Fig. 1(c). The current through the sensor is measured under constant bias ($V_{s-d} = 2.3$ V) during a 100-s exposure to 50 ppm H_2S at room temperature (blue) and at 300 °C (red). To heat the sensor, a voltage is applied to the heater leads such that the power delivered to the heater is 40 mW, which corresponds to 300 °C according to manufacturer calibration. At room temperature, the sensor response to H_2S is extremely small ($\ll 1$ nA) with long response and recovery times ($\gg 100$ s). In stark contrast, the sensor's response at 300 °C is over 500 times larger with a dramatically faster response time ($t_{50} = 0.7$ s, $t_{75} = 1.8$ s).

The sensor reported here can be thought of as a miniaturization of conventional SMO sensors. However, the nanostructured nature of the sensing element has the added advantage of much higher surface area and can be thermally cycled using very little power and without suffering from fatigue. This allows the sensor to be heated in short pulses, which decreases the overall power consumption of the device.

Figure 2 shows data from a WO_3 nanoparticle network sensor in the presence of different H_2S concentrations while being heated for 1 s every 6 s. Figure 2(a) shows the conductance versus time of the nanoparticle sensor while operating in heat-pulse mode as it is exposed to 0 and 30 ppm H_2S . The nanoparticle sensor begins to respond as soon as the sensor is exposed to H_2S (marked by the dotted line) and has come to within 25% of its final value after the first heat pulse (6 s) and within 95% of its final value after only 4 pulses or about 25 s. The nanoparticle sensor responds faster than the reference sensor making the intrinsic response time of the sensor difficult to decouple from the system response time. This shows that the WO_3 nanoparticle sensor can be operated in this heat pulse mode without significantly degrading the sensor response speed or magnitude. The average power consumed by the sensor operated in heat-pulse mode is less than 10 mW. The duration of the heat pulses have been decreased to 300 ms (data not shown) with similar results. The duration of this heat pulse can be decreased further since the calculated thermal response time of the sensor is only about 1 ms.

Figure 2(b) shows the microheated WO_3 nanoparticle-based H_2S sensor conductance versus time operating in heat-pulse mode during exposure to 10, 20, 50, 100, 150, 200, and 0 ppm H_2S , respectively. The sensor responds to changes in H_2S concentration within a few heat pulses and with clearly distinguishable response magnitudes for different concentrations. The sensor response during concentration plateaus are not completely flat, due to a slow increase in the delivered H_2S during the segment, which can be seen in the reference sensor data. Figure 2(c) shows the average nanoparticle-based sensor current in the heated state during each concentration plateau (defined as the last 7 min of the 10-min segment) versus reference sensor reading during that plateau. The monotonic response curve shows that the nanoparticle-based sensor can measure H_2S in the entire range relevant to industrial and safety applications. The nanoparticle-based sensors also have a very low coefficient of variance (CV), i.e., the standard deviation divided by the mean, as shown in Fig. 2(d). The CV of the nanoparticle-based sensor reported here is comparable to that of the much more expensive and power hungry chemiluminescence sensor. These nanoparticle-based sensors have been heated tens of thousands of times during testing without showing response degradation.

While it is intriguing to realize a low-power sensor is able to detect H_2S as low as 1 ppm (see supplemental material²⁵ for sub-ppm H_2S detection data, Fig. S1), a commercially useful sensor must be able to discriminate between the intended gas and interfering gases. To test the cross-sensitivity of the microheated WO_3 nanoparticle sensor, we chose three gases expected to be seen during operation in the natural gas industry: methane—the major component of natural gas, hydrogen, and the ever-present water vapor. Figure 3 shows the conductance versus time during five 1-s heat pulses of a WO_3 nanoparticle sensor while being exposed to different environments: 5 ppm H_2S , 13000 ppm H_2O (or 40% relative humidity at room temperature), and 5000 ppm CH_4 . The response to 5 ppm H_2S is shown as a comparison to the sensor's response to water and methane. The nanoparticle conductance during the unheated state is affected by the presence of the water. However, once the

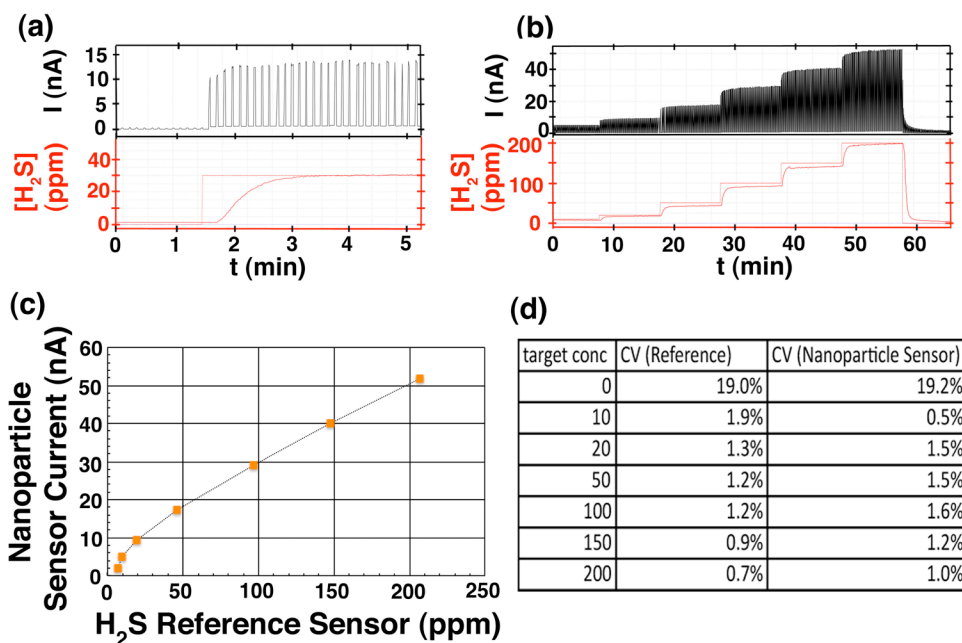


FIG. 2. Microheated WO_3 nanoparticle sensor operating in heat-pulse mode. (a) Nanoparticle sensor conductance while heat pulsing to 300°C for 1 s every 6 s during exposure to 0 and 30 ppm of H_2S . (b) Sensor conductance during heat-pulse operation when exposed to 10, 20, 50, 100, 150, 200, and 0 ppm H_2S , respectively. (c) Average sensor current reading versus average reference sensor reading for data shown in (b). Note: data during the first 3 min of the 10-min segment were not included in the analysis since the system had not reached steady state. (d) Table showing the coefficient of variance (CV), defined as the standard deviation divided by the average, of the chemiluminescence reference sensor and the heated state current of the nanoparticle-based sensor for each of the concentration set points in (b).

sensor is heated, the conductance drops to virtually zero. In the unheated state, there is some adsorbed water on the surface of the sensor creating a network of water, thereby increasing the conductance slightly, possibly due to electrochemical reactions. When the sensor is heated, we believe the water is driven off the surface and the conductance drops to almost zero.²³ Since the sensor reading is taken during the heated state, water has no direct effect on the sensor reading. The sensor conductance in the presence of methane shows absolutely no response. The microheated nanoparticle-based sensor does respond to hydrogen, but the sensitivity to hydrogen is about 0.03% of the sensitivity to hydrogen sulfide (see supplemental material²⁵ for H_2 sensing data, Fig. S2). We have shown that there is little direct response to gases other than H_2S . Obviously, a practical sensor would need to measure H_2S in the presence of these other gases. It has not yet been tested whether this sensor can operate in these more complex environments.

Here we discuss the sensing mechanism of the WO_3 nanoparticle network based H_2S sensor. For bulk WO_3 -based H_2S sensors, it has been proposed that the H_2S can either (1) reduce adsorbed oxygen or (2) donate a fraction of the sulfur lone pair electrons to the nanoparticle or (3) exchange sulfur with oxygen in the nanoparticle.²⁴ If the sensing mechanism were based on the reduction of surface adsorbed oxygen (mechanism 1), one would expect a strong response from hydrogen and a moderate response from methane. This is not

the case. Furthermore, the speed of response is much faster than that would be expected from anion exchange within the nanoparticle lattice (mechanism 3).

We believe that the underlying sensing mechanism for this WO_3 nanoparticle-based H_2S sensor does come from electron donation from the H_2S to the WO_3 nanoparticles (mechanism 2 from above). When H_2S donates electrons to the WO_3 , impurity states are filled, increasing the Fermi energy. With higher concentrations of H_2S more impurity states are filled, and the Fermi energy correspondingly increases. Since tungsten oxide is an n-type semiconductor,¹⁶ as the Fermi energy increases, the barrier height for electrons to be excited into the conduction band decreases, and, therefore, the number of thermally excited carriers increases. This causes the resistance of the nanoparticles and therefore the network as a whole to decrease.

Water does not affect the sensor the way hydrogen sulfide does even though the two molecules are very similar in structure. This is because oxygen is much more electronegative than sulfur, so the lone pairs on oxygen in water are much more tightly bound to the molecule than the lone pairs on sulfur in hydrogen sulfide. Therefore, when hydrogen sulfide adsorbs on the surface of a nanoparticle, it donates some fraction of its electrons to the nanoparticle, whereas water does not.

To determine whether the proposed sensing mechanism is consistent with the electrical transport data, let us compare

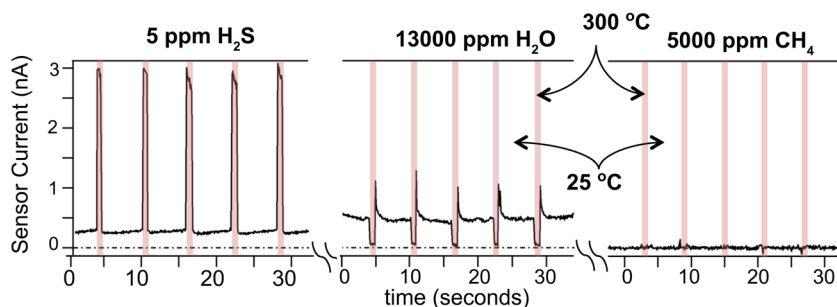


FIG. 3. Sensor current vs. time for exposures to 5 ppm H_2S , 13 000 ppm H_2O , and 5000 ppm CH_4 . Shaded areas indicate when the heater is on. Tick marks indicate 5-s intervals. During exposure to 13 000 ppm H_2O (or 40% relative humidity at room temperature), sensor current during heating is very low, indicating very little cross-sensitivity to humidity. Sensor has very little to no response to 0.5% CH_4 .

the conductance of the nanoparticle network at room temperature to that at 300 °C for each H₂S concentration. The conductivity σ of the nanoparticle is given by $\sigma = ne\mu$, where n is the number of charge carriers, e is the elementary charge, and μ is the mobility of the charge carriers. For argument's sake, we assume that the nanoparticles are in ohmic contact with one another and the electrical leads and that the mobility is constant with temperature. Then, the conductance of the nanoparticle network would be proportional to the number of charge carriers n . Since the conductance of the network is higher in the heated state than in the non-heated state for all H₂S concentrations, the carriers must be thermally activated. The charge carrier concentration n is approximately proportional to $e^{(E_f - E_c)/k_b T}$, where E_f is the Fermi energy, E_c is the conduction band edge, k_b is the Boltzmann constant, and T is the absolute temperature. Therefore, from the ratio of the nanoparticle network conductance at room temperature and at 300 °C, the difference between E_c and E_f can be determined for each H₂S concentration. The excitation barrier decreases with increasing H₂S concentration (data not shown), which is consistent with electrons filling defect states causing the Fermi level to increase.

We have shown operation of a fast, low-power, sensitive, selective microheated nanoparticle network gas sensor. The WO₃-nanoparticle-based hydrogen sulfide gas sensor reported here has a response time of a few seconds, limited or no direct sensitivity to water, methane, or hydrogen, consumes less than 10 mW of power and can be fabricated at low cost in large quantities. The sensing mechanism is believed to be related to electron donation from the H₂S to the WO₃, which causes the Fermi energy to increase, creating more charge carriers in the nanoparticle and, thereby, decreasing the sensor resistance. While the research presented here emphasizes on hydrogen sulfide sensing, this sensor platform can be used for many other gases of interest by tailoring the sensing nanomaterials to the analyte of interest.

The authors thank Eni S.p.A and the National Science Foundation-supported Center of Integrated Nanomechanical Systems (COINS) under Grant No. EEC-083819 for supporting the design and execution of the experiment. Additional electron microscopy characterization and lithographic pat-

terning support was provided by the Director, Office of Energy Research, Office of Basic Energy Sciences, Materials Sciences and Engineering Division, of the U.S. Department of Energy under Contract No. DE-AC02-05CH11231.

- ¹N. Yamazoe, *Sens. Actuators B* **108**(1–2), 2–14 (2005).
- ²E. Bakker and Y. Qin, *Anal. Chem.* **78**(12), 3965–3983 (2006).
- ³B. Benham, in The 2008 Saudi Arabia International Oil & Gas Conference & Exhibition, Dammam, Saudi Arabia, 17–19 November 2008.
- ⁴G. Y. Zhu, S. C. Zhang, H. P. Huang, Y. B. Liang, S. C. Meng, and Y. G. Li, *Appl. Geochem.* **26**(7), 1261–1273 (2011).
- ⁵M. N. Hughes, M. N. Centelles, and K. P. Moore, *Free Radic. Biol Med.* **47**(10), 1346–1353 (2009).
- ⁶R. J. Reiffenstein, W. C. Hulbert, and S. H. Roth, *Annu. Rev. Pharmacol.* **32**, 109–134 (1992).
- ⁷G. Eranna, B. C. Joshi, D. P. Runthala, and R. P. Gupta, *Crit. Rev. Solid State Mater. Sci.* **29**(3), 111–188 (2004).
- ⁸E. Comini, *Anal. Chim. Acta* **568**(1–2), 28–40 (2006).
- ⁹G. Eranna, B. C. Joshi, D. P. Runthala, and R. P. Gupta, *Crit. Rev. Solid State* **29**(3–4), 111–188 (2004).
- ¹⁰S. M. Kanan, O. M. El-Kadri, I. A. Abu-Yousef, and M. C. Kanan, *Sensors* **9**(10), 8158–8196 (2009).
- ¹¹C. M. Ghimbeu, M. Lumbreras, J. Schoonman, and M. Siadat, *Sensors* **9**(11), 9122–9132 (2009).
- ¹²N. Yamazoe, G. Sakai, and K. Shimanoe, *Catal. Surv. Asia* **7**(1), 63–75 (2003).
- ¹³G. F. Fine, L. M. Cavanagh, A. Afonja, and R. Binions, *Sensors* **10**(6), 5469–5502 (2010).
- ¹⁴H. M. Lin, C. M. Hsu, H. Y. Yang, P. Y. Leeb, and C. C. Yang, *Sens. Actuators B* **22**(1), 63–68 (1994).
- ¹⁵I. Ruokamo, T. Karkkainen, J. Huusko, T. Ruokanen, M. Blomberg, H. Torvela, and V. Lantto, *Sens. Actuatur B* **19**(1–3), 486–488 (1994).
- ¹⁶D. J. Smith, J. F. Vetelino, R. S. Falconer, and E. L. Wittman, *Sens. Actuators B* **13**(1–3), 264–268 (1993).
- ¹⁷C. S. Rout, M. Hegde, and C. N. R. Rao, *Sens. Actuators B* **128**(2), 488–493 (2008).
- ¹⁸S. Pokhrel, C. E. Simion, V. S. Teodorescu, N. Barsan, and U. Weimar, *Adv. Funct. Mater.* **19**(11), 1767–1774 (2009).
- ¹⁹V. V. Sysoev, E. Strelcov, M. Sommer, M. Bruns, I. Kiselev, W. Habicht, S. Kar, L. Gregoratti, M. Kiskinova, and A. Kolmakov, *ACS Nano* **4**(8), 4487–4494 (2010).
- ²⁰P. H. Rogers and S. Semancik, *Sens. Actuators B* **158**(1), 111–116 (2011).
- ²¹A. Friedberger, P. Kreisl, E. Rose, G. Muller, G. Kuhner, J. Wollenstein, and H. Bottner, *Sens. Actuators B* **93**(1–3), 345–349 (2003).
- ²²S. Skarupo, *EE-Eval. Eng.* **46**(6), 44+ (2007). ISSN: 0149-0370.
- ²³C. N. Xu, K. Miyazaki, and T. Watanabe, *Sens. Actuators B* **46**(2), 87–96 (1998).
- ²⁴E. P. S. Barrett, G. C. Georgiades, and P. A. Sermon, *Sens. Actuators B* **1**(1–6), 116–120 (1990).
- ²⁵See supplemental material at <http://dx.doi.org/10.1063/1.3703761> for sub-ppm H₂S detection data (Fig. S1) and for H₂ sensing data (Fig. S2).